IOP Conf. Series: Journal of Physics: Conf. Series **1037** (2018) 072007 doi:10.1088/1742-6596/1037/7/072007

High speed PIV measurements of an adaptive camber airfoil under highly gusty inflow conditions

T.T.B. Wester[1], G. Kampers[1], G. Gülker[1], J. Peinke[1], U. Cordes[2], C. Tropea[2], M. Hölling[1]

[1]ForWind - Institute of Physics, University of Oldenburg, 26111 Oldenburg, Germany
[2]Institute of Fluid Mechanics and Aerodynamics, Technical University of Darmstadt, Darmstadt, 64287, Germany

E-mail: tom.wester@uni-oldenburg.de

Abstract. Studies of the impact of gusty inflow on an adaptive camber airfoil were performed. The adaptive camber airfoil was developed at the TU Darmstadt and uses a mechanically coupled leading and trailing edge for passive load reduction.
In the present study wind tunnel experiments were performed with tailored inflow generated by means of an active grid. The main goal is the investigation of dynamic loads on such a wind turbine blade and the resulting aerodynamics around it. Therefore, temporal highly resolved PIV measurements at the suction side of the airfoil were performed. To link the local measured aerodynamics to global forces, force balances were used.

1. Introduction

A wind turbine operates in very harsh environments exhibiting large inflow velocity fluctuations on timescales of seconds. In the rotating system such inflow fluctuations result in high angle of attack (AoA) fluctuations for the turbine blade. Typical periodic inflow changes are tower passing or incoming gusts. Such variations in AoA are directly connected to lift and drag acting on the airfoil and cause dynamic force fluctuations, which may result in fatigue of the blade. Such fatigue subsequently reduces the lifetime of a wind turbine and causes additional maintenance costs. This process will further increase with in the future upscaling of the rotors. Hence it is desirable to alleviate the force fluctuations due to inflow fluctuations to reduce the cost of maintenance and thereby to increase the competitiveness of wind power.
A very promising concept to reduce dynamic loads is the adaptive camber airfoil (ACP) developed by B. Lambie and K. Hufnagel [1] at TU Darmstadt. The airfoil has a coupled leading and trailing edge flap (TEF), which enables the airfoil to decamber with increasing lift force. This leads to a less steep lift curve and thereby to a reduction of force fluctuations for AoA changes [2].
In this study a Clark-Y airfoil equipped with the adaptive camber mechanism is investigated for the first time with high speed PIV under two-dimensional AoA changes. These reproducible AoA fluctuations are created by means of an active grid in the wind tunnel and allow the investigation of the ability of the airfoil to reduce large excursions in lift forces.

2. Experimental Setup

2.1. Wind tunnel

The experiments are performed in the wind tunnel of the University of Oldenburg. The setup is shown in figure 1. The wind tunnel has a closed test section of $(0.8 \times 1.0)\,\mathrm{m}^2$ (height $\times$ width) and a length of 2.6 m. The airfoil is mounted vertically in the middle of the test section 1.1 m downstream from the nozzle and its suction side is pointing towards the observer. The active grid, which is used to generate defined AoA variations, is attached to the nozzle. The grid consists of nine vertical axes, which can be moved individually by stepper motors. This allows the generation of repeatable customized flows with required shape and statistics. The flaps are flat plates which cover the entire height of the wind tunnel. This guarantees a homogeneous inflow over the span of the airfoil and three-dimensional flow effects of the inflow can be neglected.
To investigate integral forces, two force balances of the type $K3D120$ and a torque sensor type $TS110$ from $ME-Messsysteme$ are used. The force balances are attached to the top and bottom support of the airfoil, while the torsion is only measured at the top. To understand the aerodynamic response of the airfoil in more detail time-resolved stereoscopic PIV measurements are performed at the suction side of the airfoil. The PIV system consists of two *Phantom Miro 320S* cameras with 12 GB RAM each, a *Litron 303HE* laser with a pulse energy of 22.5mJ and a *LaVision PTU*. The PIV data are measured with a sampling rate of $f_{s,PIV} = 500\,\mathrm{Hz}$ at a resolution of $(1664 \times 944)\,\mathrm{px}^2$. The field of view has a size of roughly $(440 \times 260)\,\mathrm{mm}^2$ with a spatial resolution of $(1.12 \times 1.12)\,\mathrm{mm}^2$. Due to the limited camera RAM a PIV measurement only contains 2600 double frames covering a time of 5.2s. To guarantee synchrony between all measurements and the grid movement, the PIV and force measurements are triggered by the grid movement.
To study the airfoil under realistic inflow conditions, a typical "Mexican Hat" shaped gust [3] is generated. Such a gust results in a "Mexican Hat" shaped AoA variation for a rotating airfoil.

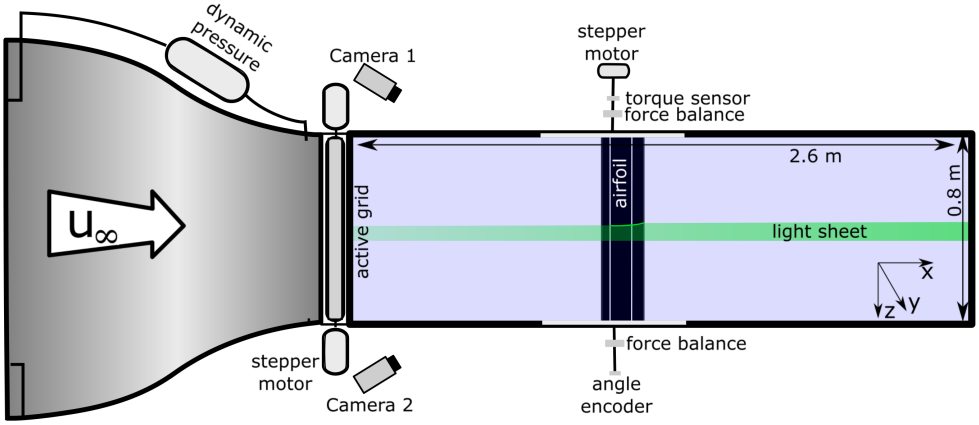

Figure 1. Experimental setup with wind tunnel, active grid, PIV system and force sensors.

2.2. Adaptive camber profile (ACP)
The Clark-Y airfoil used in the present study has a chord length of $c = 0.18\,\mathrm{m}$ and a span of $s = 0.805\,\mathrm{m}$. This profile is equipped with the adaptive camber concept and is referred to as "flexible" case or ACP. The normal Clark-Y shape, meaning the same airfoil with fixed mechanism, is referred to as "rigid". Due to the mechanically coupled leading and trailing edge, the profile can react to changing inflow conditions. For increasing pressure difference between pressure and suction side the airfoil decambers and reduces the lift force. For positive angels of the trailing edge flap (TEF), the airfoil is decambered and for negative angles the profile is cambered.
The effectiveness of the airfoil has already been investigated under steady [1] and periodic inflow conditions [4, 5]. Also numerical simulations have verified the response of the profile [6, 7]. High speed PIV together with force measurements for 2D gusty inflow have not yet been performed.

3. Results
3.1. Inflow
The first step is to examine the inflow generated by the active grid. To create a defined inflow condition control protocols for the grid are used, which contain information about the movement of each axis of the grid.
To characterize the generated inflow, X-wire measurements with a sampling frequency of $f_{s,HW} = 20 \times 10^3$Hz are performed. The X-wire is positioned at the centerline of the empty wind tunnel at the intended leading edge position of the airfoil. In order to gain spatial information of the inflow, high speed PIV measurements of the empty wind tunnel in a horizontal plane ($x-y$ plane) are performed.
For the measurements, the inflow velocity is set to $u_\infty = 14\,\frac{m}{s}$, which corresponds to a Reynolds number of $Re = 175 \times 10^3$ based on the profile's chord length. The Mexican Hat shaped inflow variation was repeated with a frequency of $f = 0.625\,Hz$, resulting in a mean angle of inflow (AoI) fluctuation from $-3.5°$ to $6°$ as shown in figure 2, where the inflow angle is plotted over time. The AoI generally describes the angle between the x and y component of the flow without reference to the chord of the airfoil. The plot also contains a phase average of the hot wire data shown in dark red, the AoI results extracted from the PIV measurement along a line at $y = 0$ (see figure 3 black line) and the used control protocol for the centerline axis of the active grid in light blue. The figure shows that all data are in good agreement. The PIV data collapse with the X-wire measurement and the flow follows the movement of the active grid axis.
Figure 3 shows the spatial AoI from the PIV data in y direction over time. These data are extracted at the position. The time series only contains three repetitions of the Mexican Hat due to the limited duration of the PIV measurement. Nevertheless it can be seen, that the inflow is homogeneous along the y-direction for all three repetitions of the Mexican Hat. This indicates a homogeneous inflow condition over a wide range of the test section.

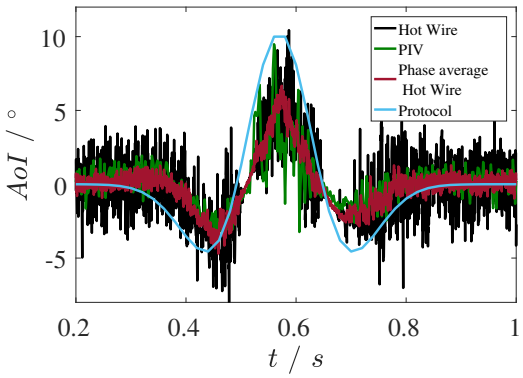

Figure 2. Measured inflow from PIV and hot wire, as well as the protocol for active grid movement.

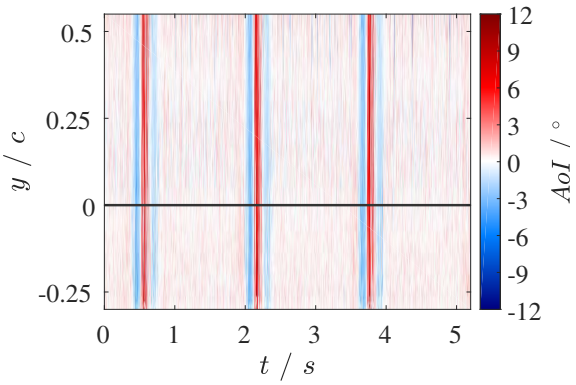

Figure 3. Spatial AoI variation extracted from PIV measurements at constant.

3.2. Aerodynamic Forces

After the inflow has been characterized, the response of the different airfoil configurations were investigated, using a fixed geometric AoA of 10°, where the geometric AoA is the angle of airfoil chord relative to the x-axis. The resulting fluctuation of the lift coefficient $\Delta C_L = C_L - \overline{C_L}$ for the rigid and flexible case is shown in figure 4, where the time axis matches with figure 2. The mean C_L is subtracted since the main goal is the damping of force fluctuations. The data are phase averages of 37 Mexican Hat periods. First of all ΔC_L is following the variation of AoI, as expected. The figure also contains markings of the maximal ΔC_L and their relative reduction to one another. Also the movement of the TEF of the airfoil is added as black dotted line for the flexible and black dashed line for the rigid case as reference.

The comparison of both lift fluctuations shows directly a reduction for the flexible case. The maximal value reached of the flexible airfoil is $\Delta C_L = 0.191$ compared to $\Delta C_L = 0.239$ for the rigid airfoil. This corresponds to a damping of 20% of the maximal fluctuation. Furthermore, the standard deviation over the complete time series changes from 0.060 for the rigid airfoil to 0.046 for the ACP, meaning a reduction of 23% in the overall fluctuations. This shows that the ACP can dampen small fluctuations in addition to large gusts.

The reason for the reduction in fluctuations is also shown in figure 4, indicating that the ACP mechanism responds similarly to the inflow. The TEF angle of the ACP changes also in a Mexican Hat shaped way, but slightly delayed compared to the acting forces. Looking at the forces it can be seen that they collapse (up to $t = 0.4s$) until the ACP mechanism begins to work. When the profile cambers ($TEF < 0$) the lift increases compared to the rigid case ($t \approx 0.45$s). Since the AoI changes from negative to positive, the lift begins to increase for both cases, which leads to a decambering of the ACP ($TEF > 0$). The fast decambering causes an earlier maximum C_L for the flexible airfoil and then a reduction of the lift back towards the mean, while the C_L of the rigid airfoil still increases up to the point where the AoI begins to decrease. The reduction of the AoI induces then an abrupt drop of the lift. This drop is much higher for the rigid airfoil than for the ACP, due to the maximum reached C_L.

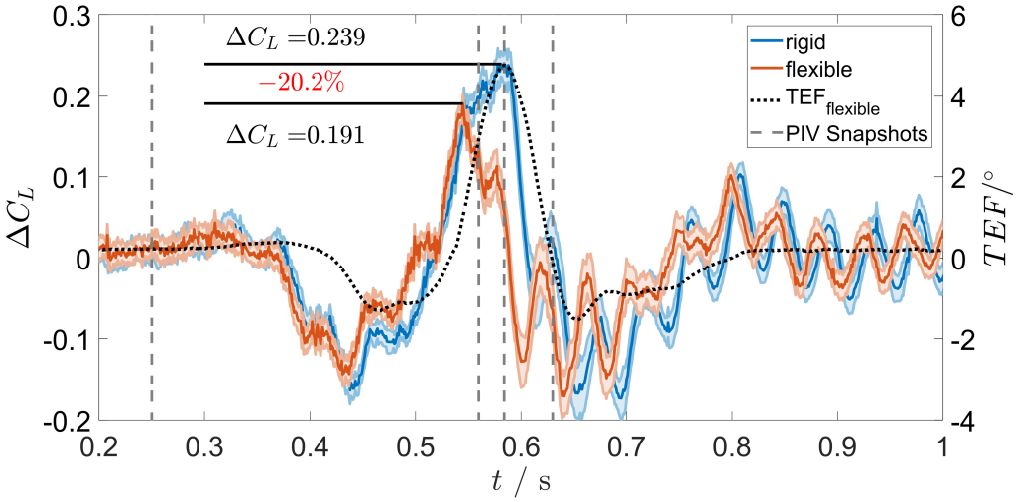

Figure 4. Phase averaged fluctuations of the lift coefficient of rigid (blue) and flexible (red) airfoil for Mexican Hat shaped inflow with standard deviation plotted as errortubes. Also plotted is the movement of the trailing edge flap (TEF) in black.

3.3. Particle Image Velocimetry

The next step is to link the integrated forces discussed in the previous section to the aerodynamic effects, using the high speed PIV measurements. Figure 5 shows four snapshots for different flow situations during the gust for every profile type. The times of the measurements are also marked in figure 4 by vertical dashed lines. The pictures on the left show the rigid airfoil and the right the flexible case. For the ACP case the rigid reference airfoil is also plotted as red edgings. Time increases from the top towards the bottom of the figure.

The first snapshots are taken before the gust hits the airfoil. Both airfoils have the same shape and the flow around the airfoils is comparable. The flow is slightly detached from both trailing edges, but this effect is not significant.

This changes for the snapshots shown in the second line. The flow detaches more for the flexible case. This coincides with figure 4, because the lift force of the flexible airfoil drops off compared to the rigid case at this time. This is due to the TEF, which is already slightly deflected upwards, as the lift force increases. Compared to this the separation area of the rigid airfoil is smaller, which results in a further increasing lift for the rigid case, whereas the flexible had already passed its maximum lift.

At the third snapshot the maximum lift for the rigid airfoil is obtained. The PIV images show that a backflow area is forming at the trailing edge of the airfoil. This backflow induces a stall of the airfoil and thereby a strong drop in lift. This can also be seen in figure 4, where the lift decreases rapidly, after the maximum is reached. In comparison to this, the ACP reaches the maximal deflection of leading and trailing edge at this time. Furthermore, this deflection of the TEF induces a deflection of the airfoil wake and of the separated flow, but compared to the snapshot before the separation has not grown further for this airfoil. This shows that a further separation of the flow is prevented by the adaptive camber mechanism and the flow becomes stabilized.

The last snapshots show the flow situation for both airfoils immediately after the maximum of the gust has passed. By comparing both separation areas of the airfoils it can be seen that the flow for the ACP is already recovering and is nearly as attached as in the first snapshot. In

contrast, the flow of the rigid airfoil is still detached significantly, which means that the flow is not in a stable state again.

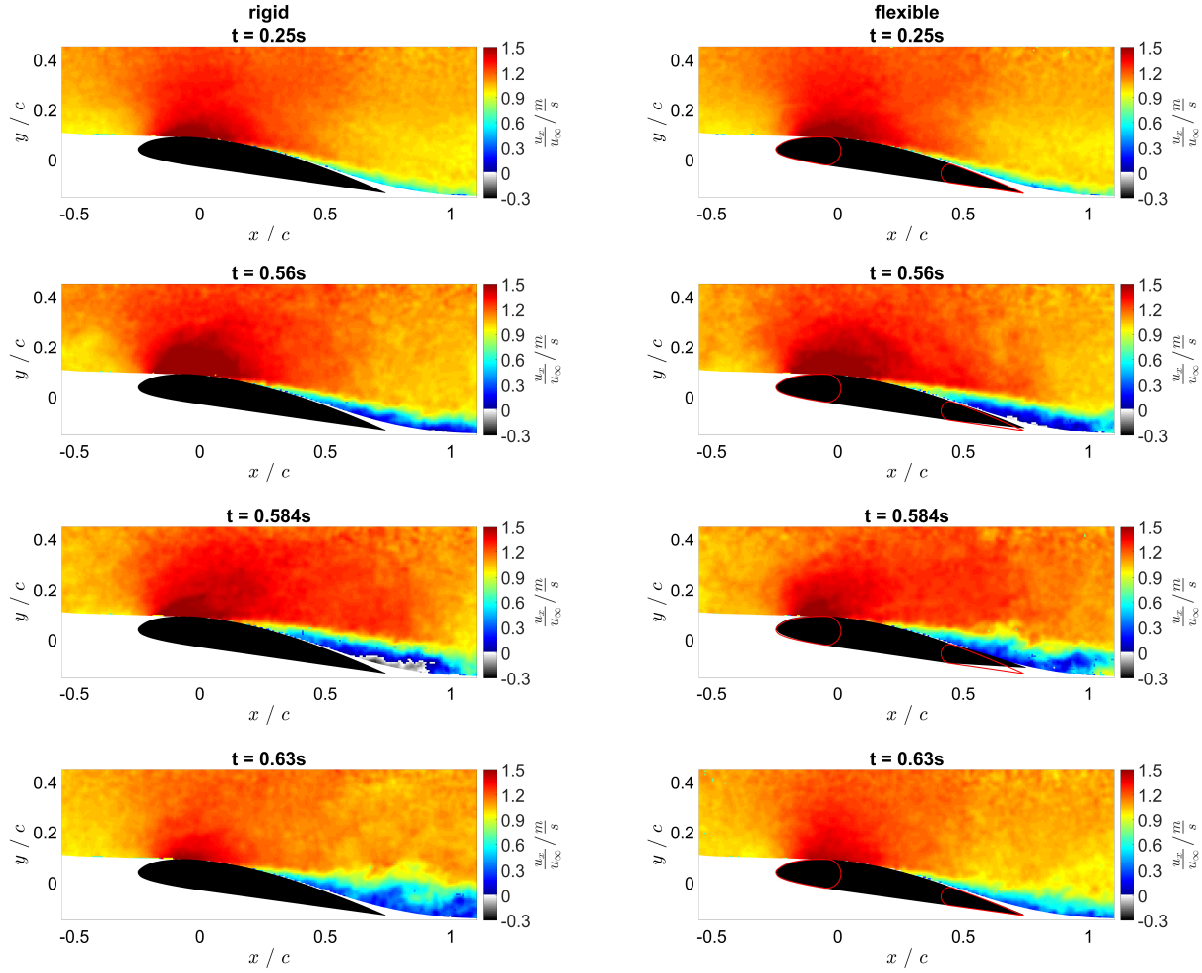

Figure 5. PIV snapshots for different flow situations (marked in figure 4) for rigid and flexible case. For the flexible case the rigid leading and trailing edge is plotted for reference with red lines.

In summary, the PIV results agree with the measured forces. They show that the ACP reacts to a gust and the mechanism dampens a separation of the flow, resulting in a flow stabilization around the airfoil compared to a rigid airfoil.

4. Conclusion

In this study it could be shown that the ACP responds directly to a given inflow. Due to the coupled leading and trailing edge, lift peaks can be reduced significantly for suddenly occurring changes in AoA. The direct comparison of the rigid and flexible airfoil had shown significant differences in the aerodynamics, as visualized using high speed PIV measurements. These measurements provided insight into how the flow around the airfoil becomes stabilized by the deflection of the TEF. Furthermore, all local effects which were captured by PIV were in good agreement with the measured integrated forces. Overall the high reduction of 20% in lift fluctuation indicates a high potential of this concept and therefore its use in wind power production.

Acknowledgments
The present investigations were performed within the DFG PAK 780 project. The authors gratefully acknowledge the German Research Foundation (DFG) for funding the studies.
We also acknowledge the Ministry for Science and Culture of Lower Saxony for the support through the funding initiative "Niedersächsisches Vorab" (project ventus efficiens).
The authors additionally want to acknowledge A. Abdulrazek, A. Fuchs and D. Traphan for helpful discussions.

References
[1] Lambie B 2011 *Aeroelastic investigation of a wind turbine airfoil with self-adaptive camber* Ph.D. thesis Technische Universität
[2] Cordes U, Lambie B, Hufnagel K, Spiegelberg H, Kampers G and Tropea C 2018 *Journal of Wind Engineering & Industrial Aerodynamics* (accepted for publication)
[3] TC88-MT I 2005 *International Electrotechnical Commission, Geneva*
[4] Cordes U, Hufnagel K, Tropea C D, Kampers G, Hölling M and Peinke J 2015 Experimental investigation of passive load reduction under dynamic inflow conditions *33rd AIAA Applied Aerodynamics Conference* p 3313
[5] Kampers G, Cordes U, Tropea C D, Hoelling M and Peinke J 2015 Stochastic analysis of aerodynamic forces acting on a self-adaptive camber airfoil in turbulent inflow *33rd AIAA Applied Aerodynamics Conference* p 2427
[6] Jost E, Fischer A, Lutz T and Krämer E 2014 Cfd studies of a 10 mw wind turbine equipped with active trailing edge flaps *10th EAWE Ph. D. Seminar on Wind Energy in Europe, Orlans* pp 51–54
[7] Fischer A, Lutz T, Kramer E, Cordes U, Hufnagel K, Tropea C, Kampers G, Hölling M and Peinke J 2016 Numerical and experimental investigation of an airfoil with load control in the wake of an active grid *Journal of Physics: Conference Series* vol 753 (IOP Publishing) p 022036